Influence of clays on the shrinkage and cracking tendency of SCC

Xiaojian Gao [a,b,*], Shiho Kawashima [b], Xiaoyan Liu [b,c], Surendra P. Shah [b]

[a] School of Civil Engineering, Harbin Institute of Technology, Harbin 150006, China
[b] ACBM Center, Northwestern University, Evanston, IL 60208, USA
[c] School of Mechanics and Materials, Hohai University, Nanjing 210098, China

ARTICLE INFO

ABSTRACT

The influence of different types of clay on the shrinkage and cracking tendency of fly ash modified self-consolidating concrete (SCCF) for the application of slipform paving were investigated in this study. The mortar phase of each mix was tested for autogenous shrinkage, total free shrinkage under drying and restrained shrinkage cracking. The mechanical properties (flexural strength, compressive strength, and modulus) were studied to supplement the results of the shrinkage and cracking tests. The plain SCCF mix was compared against the clay-modified SCCF mixes, as well as conventional SCC and slipform concrete (SFC) mixes. The results showed that the very early-age autogenous shrinkage of SCCF mortar was increased by the addition of clays due to adsorption effects. The effects of the clays on total shrinkage under long-term drying were found to depend mainly on the pozzolanic reactivity, but these effects were very slight at low dosages of about 1% by mass of binder. The early-age cracking tendency was aggravated by the clays composed of purified magnesium alumino silicate and metakaolin, but little influenced by the clay composed of kaolinite, illite and silica. Overall, the SCC mixture modified with both fly ash and a small amount of clay showed comparable shrinkage and early-age cracking performances as conventional SFC.

© 2012 Elsevier Ltd. All rights reserved.

1. Introduction

Slipform paving is widely used for concrete pavement construction, where placing, consolidating, and finishing of fresh concrete are all done in one continuous process. It relies on the high green strength (strength in the plastic state) of freshly cast concrete, which allows it to hold its shape without any formwork as it is passed through the paving machine. Although effective and faster than previous fixed-form pavers, heavy internal vibration is necessary to cast the high-stiffness concrete designed for slipform pavers. Not only does this make slipform paving energy intensive, but oftentimes problems associated with over-consolidation, such as segregation and significant reduction of entrained air, lead to reduction in durability and extensive longitudinal cracking along the path of the vibrators [1].

There is an obvious need to modify this process to eliminate or reduce the need for internal vibration. One approach has been to design a new type of concrete that optimizes flowability, consolidation and green strength. It has been demonstrated that with proper proportioning of various mineral and chemical admixtures in self-consolidating concrete (SCC) mixtures, it is possible to perform the slipform paving process without the need for any vibration while still achieving sufficient shape stability and finish [2]. Clays, including nanoclays, were a key mineral admixture in attaining these desired properties.

Clays have a significant influence on the fresh-state properties of cementitious material. Even when added in small amounts (up to 1.5% by mass of cement), they have been found to increase green strength of concrete [3]. Although the mechanisms are not completely understood, work has shown that clays increase flocculation strength [4] and floc size [5] when added to cement paste, which would lead to an apparent increase in stiffness. Clays make it possible to modify SCC mixes so that they can achieve green strength comparable to that of typical slipform concrete (SFC) with little compromise to flowability and compactibility.

Understanding of the shrinkage and early age cracking behavior of concrete structures is important, especially for pavements with large surface areas exposed to outdoor environments and repeated heavy service loads. This has generated research interest on the influence of various mineral admixtures (fly ash, silica fume, blast furnace slag) on the shrinkage behavior of concrete, including SCC [6–9]. However, studies on the influence of small clay additions on the shrinkage of SCC are lacking, due to the novelty of the idea. Although previous work has shown the potential of clay additions in tailoring the fresh-state properties of SCC, its influence on hardened properties (i.e. shrinkage) must be understood, as well. In this study, the autogenous shrinkage, drying

shrinkage, and shrinkage induced cracking behavior of clay-modified SCC mixes were investigated. The mechanical properties (flexural strength, compressive strength, and modulus) were studied, as well, to supplement the results of the shrinkage and cracking tests.

2. Experimental

2.1. Raw materials and mixtures

Twelve mortar mixtures were investigated, shown in Table 1. The SFC, SCC and SCCF mix proportions were based on concrete mixes from previous studies [10]. (Since the coarse aggregate contents were similar between mixes, it was assumed acceptable to only test the mortar phase.) The mix design of SCC was optimized to achieve maximum flowability and segregation resistance. SCCF is SCC with a 30% replacement of cement with fly ash, which reduces its cost to that comparable of traditional SFC. The previous studies showed that the addition of 1.5% of clay by mass of binder modified the fresh-state properties of SCCF to a satisfactory condition for slipform paving without any vibration. Therefore, SCCF mixes with three dosages of clays were studied here: 1.0%, 1.5% and 2.0%.

Type I ordinary Portland cement and tap water were used in all mixes. Fly ash (Class F) and three types of clay (C1 [11], C2 [12], C3 [13]), including a calcined clay, were used as mineral additives. Details of these mineral additives are given in Table 2 and the chemical compositions of all the fine materials are given in Table 3. The plasticizer that was used for all mixtures was a naphthalene-sulfonate based superplasticizer. The aggregate was river sand with a specific gravity of 2.66 and a particle size distribution presented in Table 4.

2.2. Mixing procedure

A medium or large planetary mixer was used for every mortar mix using the following procedure: (1) add all the dry materials, mix for 3 min at low speed; (2) add water and superplasticizer, mix for 3 min at low speed; (3) scrape bowl, mix for another 4 min at high speed.

2.3. Free shrinkage test

Autogenous deformation was measured using the corrugated tube protocol based on the work of Jensen and Hansen [14] as shown in Fig. 1. The corrugated polyethylene tubes, 400 mm in length and 30 mm in diameter, were cast with fresh mortar and sealed with two end caps. The length change was then monitored according to ASTM C 1698-09 [15]. Fresh mortar was consolidated by running a vibrating rod along the length of the tube. Two specimens were prepared for each mix. Each test was carried out for 14 days in a chamber with a constant temperature of 23 °C and readings were continuously recorded every 10 min. All of the

Table 2
Mineral admixtures.

Material	Description	Mean particle size (μm)	Specific surface area (m²/g)
C1	Purified magnesium alumino silicate	65.2, 1.75[a]	150
C2	Kaolinite, illite, silica	13.0, 0.5[a]	23
C3	Metakaolin	3.54, 1.20[a]	13

[a] Highly dispersed state.

Table 3
Chemical compositions of cement and admixtures (%).

Oxide	Cement	Fly ash	C1	C2	C3
SiO_2	19.5	42.47	49.57	68.0	53.0
Al_2O_3	4.7	26.01	9.44	24.0	43.8
Fe_2O_3	2.80	8.44	3.31	2.4	0.43
CaO	64.2	14.01	1.88	0.2	0.02
MgO	2.50	3.15	8.81	0.5	0.03
SO_3	2.6	1.57	0.00	0.0	0.03

Table 4
Size distribution of sand (%).

Sieve size (mm)	9.5	4.75	2.36	1.18	0.6	0.3	0.15	0.075
Passing percent	100.0	99.3	89.1	74.8	56.7	21.1	2.6	0.6

Fig. 1. Corrugated tube for measuring autogenous shrinkage.

readings were zeroed to time of initial set. The time of initial set was determined on the paste phase by the Vicat Needle Test (a penetration test) in accordance with standard ASTM C191-08 [16].

The drying shrinkage of mortar was measured on prism specimens according to standard ASTM C157-04 [17]. The length change of 100 × 100 × 300 mm prisms were monitored over time and the drying shrinkage was expressed as a linear strain. Each specimen

Table 1
Mix proportions.

Mixture	SFC	SCC	SCCF	C1-1	C1-2	C1-3	C2-1	C2-2	C2-3	C3-1	C3-2	C3-3
Cement	100	100	70	70	70	70	70	70	70	70	70	70
Fly ash	0	0	30	30	30	30	30	30	30	30	30	30
Water	43	40	40	40	40	40	40	40	40	40	40	40
Clay												
Type	/	/	/		C1			C2			C3	
Amount	/	/	/	1.0	1.5	2.0	1.0	1.5	2.0	1.0	1.5	2.0
Sand	251	154	154	154	154	154	154	154	154	154	154	154
Plasticizer	1.0	0.39	0.39	0.39	0.39	0.39	0.39	0.39	0.39	0.39	0.39	0.39

was cast in three layers and consolidated manually after every layer. They were then covered with a plastic sheet to prevent moisture loss and demolded after 24 h. Immediately after demolding, two copper stubs were attached to a longitudinal surface with epoxy resin and allowed to set for at least 2 h before the initial measurement. The distance between the two stubs was measured using a manual strain gage, as shown in Fig. 2. The specimens were also weighed to determine the mass loss due to water evaporation. Three prisms were prepared and monitored for each mix. For the duration of the test, the prisms were kept in a condition controlled chamber set at 23 °C and 50% RH.

2.4. Restrained shrinkage test

The ring test was performed to evaluate the cracking behavior of the mortars in restrained shrinkage conditions. The test was carried out based on standard ASTM C 1581-04 [18], the setup of which is shown in Fig. 3 [19]. The steel ring acts as a passive restraint to the surrounding mortar. As the mortar undergoes shrinkage, it applies a uniform stress onto the steel leading to a strain development within the steel ring. At the same time, a tensile stress develops in the mortar ring due to the restraint of steel ring. When the stress increases to above a threshold value, the mortar cracks and the strain within
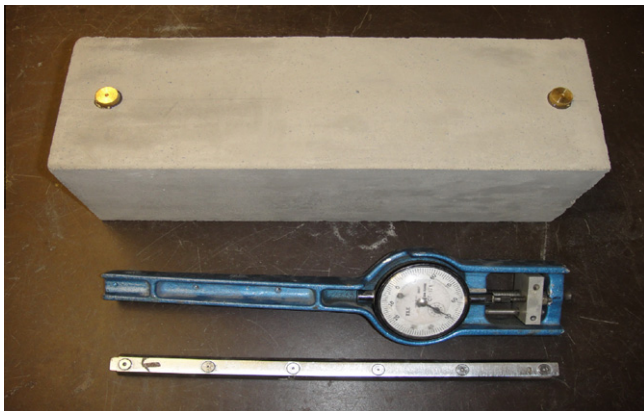
Fig. 2. Specimen and setup for drying shrinkage test.
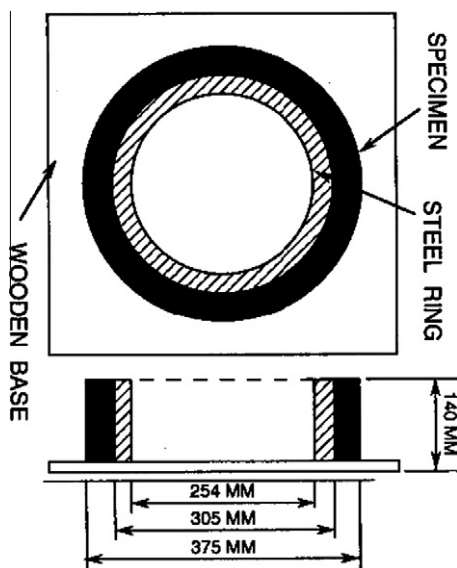
Fig. 3. Setup for the restrained ring test, including ring dimensions.

the steel ring drops significantly. Two ring specimens were cast for each mortar mixture. The specimens were cast around a steel ring by using a cardboard tube as the outside mold. Immediately after demolding, at 24 h, the top surface of the ring specimen was sealed with silicone rubber. This procedure creates a condition that allows drying only from the outer circumferential surface. The strain measurement of each steel ring was monitored from the demolding time, having subsequent readings recorded every 30 min. After initial cracking occurred, the cracking widths were measured daily by using a microscope with a precision of 2.5 μm. The results reported in this paper are the average of three measurements taken along the cracking length (top, center and bottom).

2.5. Mechanical measurements

Flexural strength tests according to ASTM C348-08 [20] were carried out on select mortar mixtures. Prism specimens with dimensions $40 \times 40 \times 160$ mm were cast in two layers, vibrated manually and finished by a steel trowel. After initial curing of 24 h or 12 h by covering the specimens with a plastic sheet at room temperature, the specimens were demolded and stored in a foggy room at a temperature of 23 ± 2 °C. For every mixture, flexural strength was measured for three specimens at ages of 0.5, 1, 3, 7, 14 and 28 days after casting. Three-point loading was performed by using the mid-span deflection control at a constant rate of 0.6 mm/min until fracture.

Compressive strength and modulus were tested on the same cylinder specimens with dimension of $Ø75 \times 150$ mm in accordance with ASTM C469-02 [21]. Three specimens were tested by using the compression strain control at a constant rate of 0.5 mm/min, and the results were obtained as the average. The casting, demoulding, curing condition and test ages for the cylinder specimens are the same as those for the flexural specimens.

3. Results and discussion

3.1. Autogenous shrinkage

The results of the autogenous shrinkage test for SFC, SCC and SCCF are presented in Fig. 4. As expected, all three mixes experienced some swelling during the first several hours. This was caused by simultaneously occurring (1) autogenous swelling induced by the creation of early hydrated products and (2) chemical shrinkage leading to self-desiccation. Swelling dominates at the beginning then decreases over time [22]. Reabsorption of bleeding water also causes an initial expansion in sealed samples,
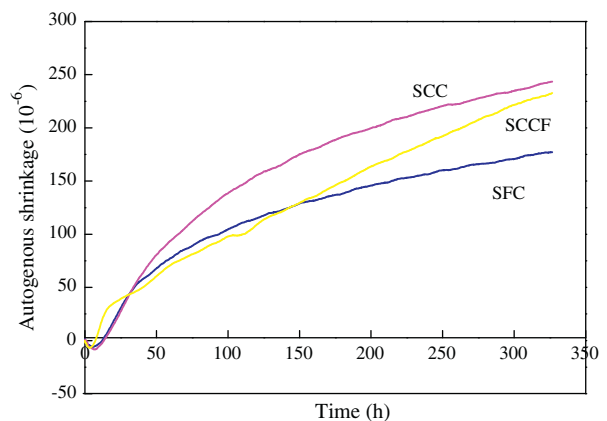

Fig. 4. Autogenous shrinkage of SFC, SCC and SCCF mortar.

which is even more pronounced than the swelling caused by the formation of hydrates [23].

SCC showed 40% higher autogenous shrinkage than SFC at 14 days. This is due to the lower w/c ratio of SCC (0.4 versus 0.43 for SFC) along with its higher cement-to-sand ratio. Typically fly ash is considered a pozzolanic material with low reactivity, effective in reducing the autogenous shrinkage of cements and concretes. However, the replacement of 30% of cement with fly ash in SCCF increased the autogenous shrinkage development during the first day. This may be attributed to increased ettringite formation and water consumption, which have been reported to occur between 2 and 5 h after mixing in fly ash–cement–water mixtures [24]. In addition, the hydration of cement particles is accelerated by the nucleation sites provided by the fly ash, as well as their dilution effect [25]. Another study showed that the autogenous shrinkage of concrete increased when the replacement of fly ash was 25%, but decreased when it was 50% [26]. After 2 days, SCCF showed a clear reduction in rate of shrinkage, went on to experience lower absolute autogenous shrinkage compared to SCC. However, the rate of shrinkage of SCC decreased with time while it stayed constant for SCCF, due to the pozzolanic effect of the fly ash. By day 14, the shrinkage of SCCF was very close to that of SCC, indicating no mitigating effect of fly ash on autogenous shrinkage longer term.

Fig. 5 presents the influence of the clays, at an addition of 2% by mass of binder, on the autogenous shrinkage of SCCF mortar. There is no initial swelling in any of the clay mixtures. This can be explained by the high specific surface area and water adsorption of the clays, which would improve the consistency of fresh mortar
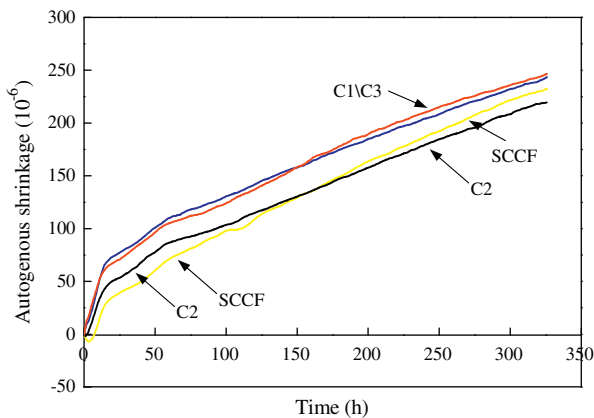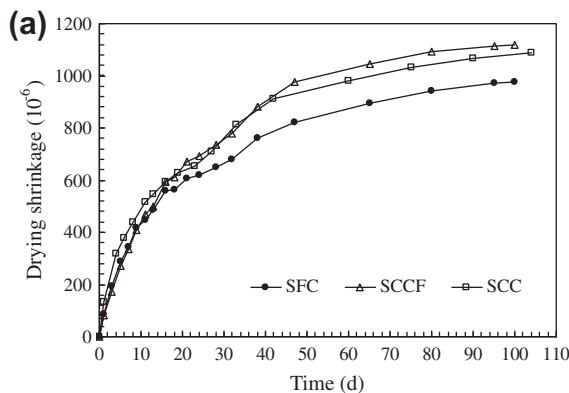
by reducing bleeding in the tube specimens. C1 and C3 increased the autogenous shrinkage overall while C2 increased the autogenous shrinkage during the first 5 days but had little influence at later ages.

The addition of C1 and C3 increased the autogenous shrinkage at very early ages but this increase became less significant over time; shrinkage strains were 10–15 microstrain higher than the control mortar at 2 weeks. C1 is a highly purified magnesium alumino silicate of uniform size and shape, with an average length of 1.5–2 μm and an average diameter of 3 nm. This fibrous clay has a high specific area of 150 m^2/g and specially charged surfaces, which allows it to easily gel and adsorb 200% water by mass [3]. This can reduce the free water-to-binder ratio from 0.4 to 0.36. This is likely the reason for the higher early-age autogenous shrinkage, which increases linearly as w/c decreases from 0.60 to 0.25 [27]. The physically adsorbed water is gradually released during cement hydration, which explains why the clay mixes experienced similar autogenous shrinkage as plain SCCF at later ages. Furthermore, metakaolin (the main composition in C3) has a higher pozzolanic reactivity and filler effect, which has been validated by the increased strength after 1 day when 5% metakaolin was used to replace cement [28]. This would refine the pore structure and likely lead to an increase in autogenous shrinkage, as observed in this study. However, in other work the replacement of cement by 5% metakaolin was reported to reduce early age autogenous shrinkage of paste with water to binder ratio of 0.5 [29]. C2 has a moderate adsorption effect and a very high fineness, which led to higher autogenous shrinkage during the first 5 days. After that, it had little influence on shrinkage, as it is composed of kaolinite, illite and silica and therefore anticipated to be inactive in cement paste.

3.2. Drying shrinkage and water loss

The total shrinkage and water loss over time of SFC, SCC and SCCF specimens under drying conditions are presented in Fig. 6. Higher shrinkage occurred in the SCC specimens than the SFC specimens during the test due to higher autogenous shrinkage (discussed in Section 3.1) and higher cement paste content. However, no measurable difference was found between the water loss curves of SCC and SFC, which maybe attributable to the following two counteracting effects: the lower w/c ratio tends to reduce the water loss and the higher paste content increases the effective surface exposure of the specimen to drying. During the first 2 weeks, shrinkage was somewhat reduced by the 30% replacement of cement with fly ash, which can be attributable to three aspects: the decreased autogenous shrinkage (see Fig. 4), the inert filler effects of fly ash to restrain shrinkage and the changed pore structure of
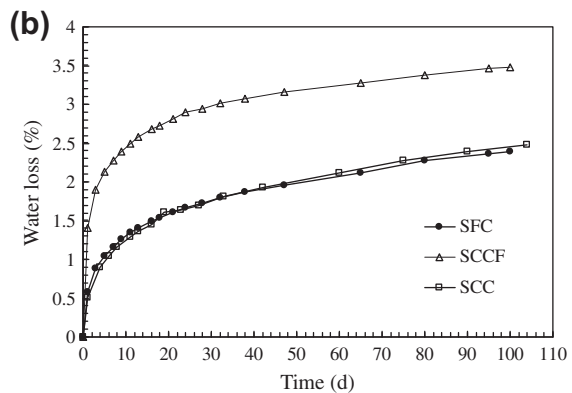

Fig. 5. Influence of different clay types (additions of 2% by binder mass) on autogenous shrinkage of mortar.

Fig. 6. Total shrinkage and water loss of SFC, SCC and SCCF specimens exposed to drying (a) shrinkage and (b) water loss.

the fly ash–cement paste. SCCF mixture with fly ash possibly has a coarser pore structure than SCC due to the coarser particle size of fly ash than cement [10] and, consequently, showed the reduced strength by more than 10% at 14 days as measured in this study. This is the most important reason for a tremendous increase in water loss observed in SCCF sample. Although the addition of fly ash did not lead to a measurable increase in shrinkage strain at early ages, aggravated desiccation in the fly ash–cement paste at later ages resulted in a slightly higher shrinkage of SCCF than SCC.

The influence of a 2% addition of clay on the drying shrinkage and water loss of SCCF are shown in Fig. 7. C1 and C2 both increased drying shrinkage and water loss. The governing factor is likely linked to the water adsorption of the clays. The physically adsorbed water on the clay particles undergo desorption from environmental drying and cement hydration, contributing to volu-

metric shrinkage [30]. On the other hand, C3 led to decreases in both drying shrinkage and water loss. C3 is composed of metakaolin, which has high pozzolanic reactivity [31]. The reduction of total shrinkage upon drying can be partly attributed to the increased difficulty of moisture transport as the hydration and pozzolanic reactions consume more free water and lead to a finer pore structure. Similar results have been observed by Brooks and Johari [32] on concrete containing 5–15% metakaolin. There is no evidence that C1 is reactive in cementitious materials and kaolinite, the main component of C2, has little pozzolanic reactivity when being calcined below 700 °C [33]. Therefore, the pozzolanic reactivity of the clays significantly influences the shrinkage behavior of drying specimens at long-term ages.

The effects of different additions (1.0–2.0%) of each clay type on the shrinkage of SCCF are presented in Fig. 8. Similar to what was
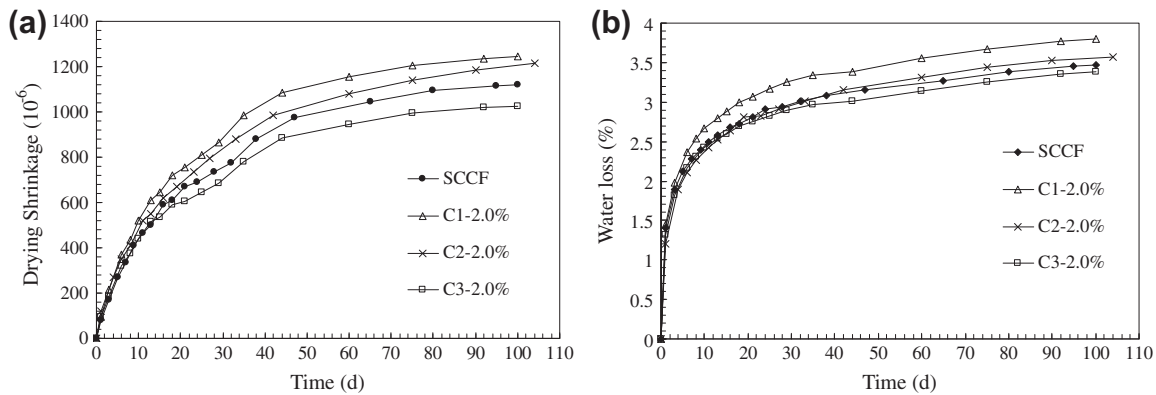
Fig. 7. Influence of different clay types on the shrinkage and water loss of mortar exposed to drying (a) shrinkage and (b) water loss.
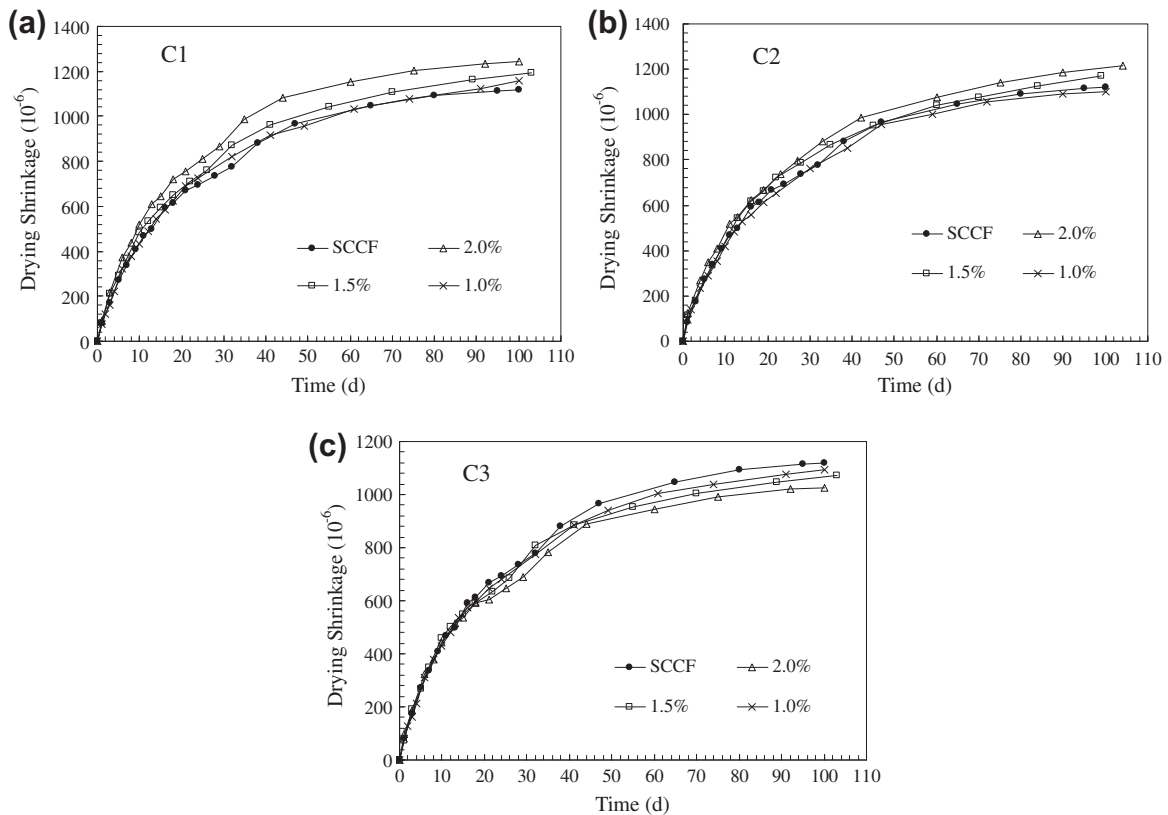

Fig. 8. Influence of different additions of clays on shrinkage of mortar exposed to drying.

shown in Fig. 7, C1 and C2 increased drying shrinkage strain while C3 decreased it. And increasing the addition content further enhanced these effects. Overall, additions of up to 1.5% for all clays did not lead to significant changes in measurable drying shrinkage strain.

3.3. Restrained ring test

The strain and crack width development of the rings without clay additions are presented in Figs. 9a and 10a, respectively. In comparison with SFC, the SCC rings showed a higher rate in strain development and a higher final strain, as well as a 25% greater final crack width. These results correlate well with those of the free shrinkage tests, where SCC specimens experienced higher total shrinkage and shrinkage development rates. The SCCF rings experienced a significant decrease in rate of strain development and a delay in cracking time by 66 h compared to the SCC rings. The 30% replacement of cement with fly ash also led to a decrease in crack width development, with a 27% reduction in final crack width. Furthermore, SCCF showed higher cracking resistance than SFC although it had a higher total free shrinkage under drying. This can be explained by the lower modulus and higher creep performances induced by the addition of fly ash [34].

At additions of 2% by mass of binder, all three clays increased strain development in SCCF, as shown in Fig. 9b. C1 and C3 mixtures had earlier cracking times (90.5 and 104.5 h, respectively) than the plain SCCF rings (123.5 h). C2 did not have as much of an effect on cracking time (118.5 h). Although the C3-2% mix experienced decreased total free shrinkage at later ages compared to SCCF (see Fig. 8c), it had an earlier cracking time. When the addition dosage was reduced to 1.5%, C1 and C3 both still led to earlier cracking, as shown in Fig. 9c. The further increase in ring strain

(compared to 2% dosage) could be attributed to the modulus development of mortar.

Fig. 10b compares the crack width development of SCCF rings against those with clay additions of 1.5% and 2.0%. C1 and C2 both had minor effects on crack width development while C3 led to a notable decrease. The results of final crack width are in good agreement with the free shrinkage results at 28 days (see Figs. 7 and 8). The early age cracking sensitivity was aggravated by the addition of C1 and C3, as indicated by the earlier cracking times. However, this did not necessarily result in greater crack growth. And C2 had no evident effect on the cracking sensitivity or crack development of mortar. Anyway, clay and fly ash modified SCC showed an improved early age cracking performance overall than SFC, which demonstrates the applicability of this new type of concrete in practice.

3.4. Mechanical performances

The influences of 1.5% addition of C1 and C3 on the mechanical properties of SCCF are shown in Fig. 11. At 12 h, the flexural strength, compressive strength and modulus were all increased by the addition of the clays due to adsorption and filler effects. At 1 day, the strengths were marginally decreased by the addition of clay. After 3 days, strength and modulus continued to decrease in C1 mixture, but increase slightly in C3 mixture. This is due to the difference in pozzolanic reactivity of each type of clay, as discussed previously.

The reduced flexural strength is another reason for the early cracking time C1 exhibited in the restrained shrinkage tests. The similar strength and modulus development of mortar with and without C3, however, is contrary to the previous results of the cracking test, where C3 rings had earlier cracking times than plain
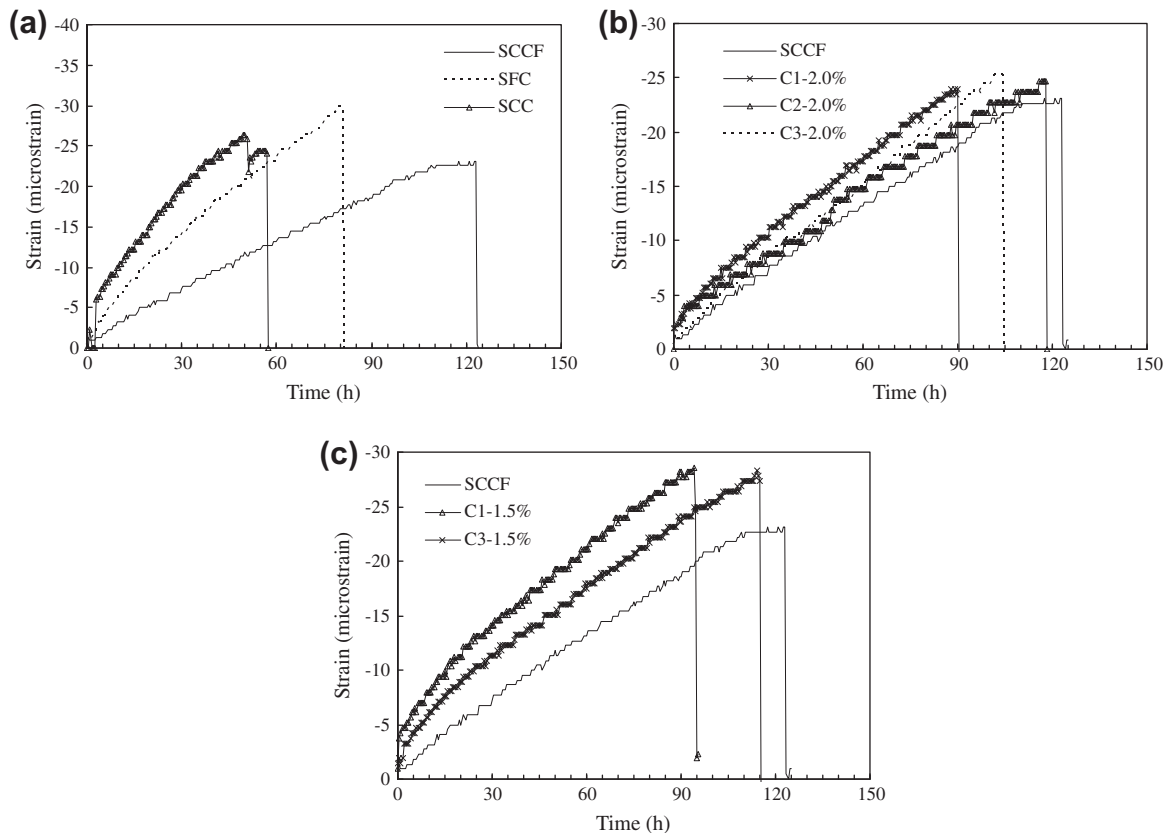

Fig. 9. The development of steel ring strain with drying time (a) no clay; (b) addition of 2% clay; (c) addition of 1.5% clay.
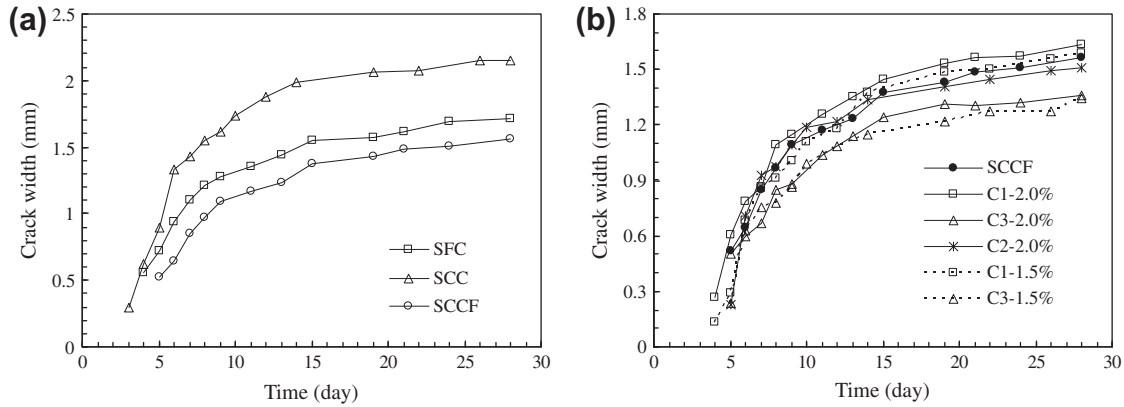
Fig. 10. Crack width development of ring specimen with drying time (a) no clay and (b) influence of different clay.
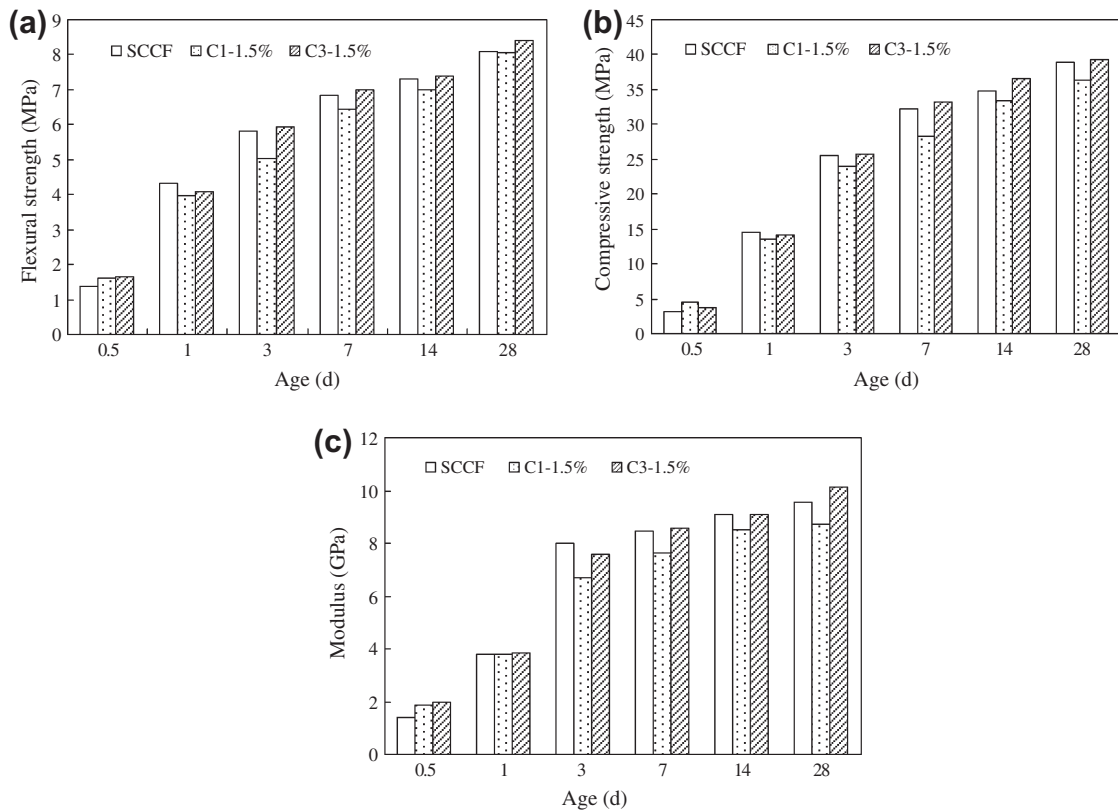

Fig. 11. Strength and modulus development with curing time (a) flexural strength; (b) compressive strength; (c) Young's modulus.

SCCF rings. The difference between curing conditions for the strength and shrinkage cracking specimens should be considered in a future study (strength specimens were moist cured while shrinkage specimens were not), along with creep performance of mortar containing clay, which is another important factor influencing early age cracking.

4. Conclusions

Fly ash and clay-modified SCC have enhanced fresh-state properties, i.e. high green strength and high initial fluidity, which lead to increased efficiency during the paving process. In this study, it was determined whether the shrinkage and cracking behavior of fly ash modified self-consolidating concrete (SCCF) with clays were comparable to that of slipform concrete (SFC), properties that are critical for paving applications. The following conclusions can be drawn from this study:

(1) SCC showed higher autogenous shrinkage and higher total shrinkage and cracking tendency under drying than conventional SFC. The addition of 30% fly ash delayed the cracking time and reduced the final crack width of SCC, although it increased water evaporation and total free shrinkage of specimens upon drying. Therefore, SCCF showed a better restrained cracking performance than SFC.

(2) All three clays slightly increased the very early age autogenous shrinkage of SCCF due to adsorption effects. At later ages, the increase was neglectable.

(3) A 2% addition by mass of binder in SCCF of C1 (clay composed of purified magnesium alumino silicate) and C2 (clay composed of kaolinite, illite, silica) led to an increase in total shrinkage under long-term drying while C3 (clay composed of metakaolin) led to a decrease. At lower additions of 1.0%, little influence on total shrinkage was measured for all clays.

(4) C1 increased cracking tendency due to higher shrinkage and decreased flexural strength development. C2 had very limited influence on the cracking time and crack width, which correlated well with the results of the free shrinkage test. C3 decreased total shrinkage and did not affect strength or modulus development. However, C3 experienced earlier cracking than plain SCCF in the restrained shrinkage tests. This may be due to the curing conditions – restrained shrinkage specimens did not undergo a period of moist curing after demolding. Factors such as creep and curing conditions should be considered in further studies.

(5) At low addition levels (up to 2%), none of the clays had a greatly adverse effect on shrinkage and early-age cracking – overall, SCC mixes modified with fly ash and small additions of clay showed comparable performance as conventional SFC.

Acknowledgments

References

[1] Ardani A, Hussain S, LaForce R. Evaluation of premature PCC pavement longitudinal cracking in Colorado. In: Proceedings of the 2003 mid-continent transportation research symposium, Ames, Iowa, USA; 2003.
[2] Pekmezci BY, Voigt T, Wang K, Shah SP. Low compaction energy concrete for improved slipform casting of concrete pavements. ACI Mater J 2007;104(3):251–8.
[3] Tregger N. Tailoring the fresh state of concrete. PhD thesis. Evanston, Northwestern University; 2010.
[4] Tregger N, Pakula ME, Shah SP. Influence of clays on the rheology of cement pastes. Cem Concr Res 2010;40(3):384–91.
[5] Ferron R. Formwork pressure of self-consolidating concrete: influence of flocculation mechanisms, structural rebuilding, thixotropy and rheology. PhD thesis. Evanston, Northwestern University; 2008.
[6] Khatib JM. Performance of self-compacting concrete containing fly ash. Constr Build Mater 2008;22(9):1963–71.
[7] Gesoglu M, Guneyisi E, Ozbay E. Properties of self-compacting concretes made with binary, ternary, and quaternary cementitious blends of fly ash, blast furnace slag, and silica fume. Constr Build Mater 2009;23(5):1847–54.
[8] Sahmaran M, Yaman IO, Tokyay M. Transport and mechanical properties of self consolidating concrete with high volume fly ash. Cem Concr Compos 2009;31(2):99–106.
[9] Guneyisi E, Gesolu M, Ozbay E. Strength and drying shrinkage properties of self-compacting concretes incorporating multi-system blended mineral admixtures. Constr Build Mater 2010;24(10):1878–87.
[10] Tregger N, Voigt T, Shah SP. Improving the slipform process via material manipulation. In: Advances in construction materials, Stuttgart, Germany; July 23–24, 2007.
[11] Active Minerals Company LLC. What is acti-gel 208 and how is it made?; 2007.
[12] Stephan Schmidte Gruppe. Technisches Datenblatt Concresol 105; 2004.
[13] Engelhard. MetaMax high-reactivity metakaolin for concrete; 2008.
[14] Jensen OM, Hansen PF. Dilatometer for measuring autogenous deformation in hardening Portland cement paste. Mater Struct 1995;28(181):406–9.
[15] ASTM C 1698-09. Standard test method for autogenous strain of cement paste and mortar. West Conshohocken, PA: ASTM International; 2010.
[16] ASTM C 191-08. Time of setting for hydraulic cement by vicat needle. West Conshohocken, PA: ASTM International; 2008.
[17] ASTM C 157-04. Test method for length change of hardened hydraulic cement mortar and concrete. West Conshohocken, PA: ASTM International; 2004.
[18] ASTM C 1581-04. Determining age at cracking and induced tensile stress characteristics of mortar and concrete under restrained shrinkage. West Conshohocken, PA: ASTM International; 2004.
[19] Sarigaphuti M, Shah SP, Vinson KD. Shrinkage cracking and durability characteristics of cellulose fiber reinforced concrete. ACI Mater J 1993;93(4):309–18.
[20] ASTM C348-08. Flexural strength of hydraulic-cement mortars. West Conshohocken, PA: ASTM International; 2008.
[21] ASTM C469-02. Static modulus of elasticity and Poisson's ratio of concrete in compression. West Conshohocken, PA: ASTM International; 2006.
[22] Barcelo L, Moranville M, Clavaud B. Autogenous shrinkage of concrete: a balance between autogenous swelling and self-desiccation. Cem Concr Res 2005;35(1):177–83.
[23] Mohr BJ, Hood KL. Influence of bleed water reabsorption on cement paste autogenous deformation. Cem Concr Res 2010;40(2):220–5.
[24] Berry EE, Hemmings RT, Cornelius BJ. Mechanisms of hydration reactions in high volume fly ash pastes and mortars. Cem Concr Compos 1990;12(4):253–61.
[25] Lawrence P, Cyr M, Ringot E. Mineral admixtures in mortars: effect of inert materials on short-term hydration. Cem Concr Res 2003;33(12):1939–47.
[26] Termkhajornkit P, Nawa T, Nakai M, Saito T. Effect of fly ash on autogenous shrinkage. Cem Concr Res 2005;35(3):473–82.
[27] Baroghel-Bouny V, Mounanga P, Khelidj A, Loukili A, RafaR N. Autogenous deformations of cement pastes Part II. W/C effects, micro–macro correlations and threshold values. Cem Concr Res 2006;36(1):123–36.
[28] Khatib JM. Metakaolin concrete at a low water to binder ratio. Constr Build Mater 2008;22(8):1691–700.
[29] Gleize PJP, Cyr M, Escadeillas G. Effects of metakaolin on autogenous shrinkage of cement pastes. Cem Concr Compos 2007;29(1):80–7.
[30] Chertkov VY. Modelling the shrinkage curve of soil clay pastes. Geoderma 2003;112(1–2):71–95.
[31] Sabir BB, Wild S, Bai J. Metakaolin and calcined clays as pozzolans for concrete: a review. Cem Concr Compos 2001;23(6):441–54.
[32] Brooks JJ, Johari MAM. Effect of metakaolin on creep and shrinkage of concrete. Cem Concr Compos 2001;23(6):495–502.
[33] Ambroise J, Murat M, Pera J. Hydration reaction and hardening of calcined clays and related minerals: V. Extension of the research and general conclusions. Cem Concr Res 1985;15(2):261–8.
[34] Siddique R. Performance characteristics of high-volume Class F fly ash concrete. Cem Concr Res 2004;34(3):487–93.